ELSEVIER

International Journal of Minerals, Metallurgy and Materials
Volume 16, Number 3, June 2009, Page 293

Materials

Antibacterial and corrosive properties of copper implanted austenitic stainless steel

Juan Xiong[1)], *Bo-fan Xu*[2)], *and Hong-wei Ni*[2)]

1) School of Physics and Electronic Technology, Hubei University, Wuhan 430062, China

2) School of Material and Metallurgy, Wuhan University of Science and Technology, Wuhan 430081, China

(Received 2008-06-24)

Abstract: Copper ions were implanted into austenitic stainless steel (SS) by metal vapor vacuum arc with a energy of 100 keV and an ions dose range of $(0.5\text{-}8.0)\times10^{17}$ cm^{-2}. The Cu-implanted SS was annealed in an Ar atmosphere furnace. Glancing X-ray diffraction (GXRD), transmission electron microscopy (TEM) and Auger electron spectroscopy (AES) were used to reveal the phase compositions, microstructures, and concentration profiles of copper ions in the implanted layer. The results show that the antibacterial property of Cu-implanted SS is attributed to $Cu_{9.9}Fe_{0.1}$, which precipitated as needles. The depth of copper in Cu-implanted SS with annealing treatment is greater than that in Cu-implanted SS without annealing treatment, which improves the antibacterial property against *S. aureus*. The salt wetting-drying combined cyclic test was used to evaluate the corrosion-resistance of antibacterial SS, and the results reveal that the antibacterial SS has a level of corrosion-resistance equivalent to that of un-implanted SS.

Key words: copper ion implantation; stainless steel; antibacterial property; corrosion resistance

[*This work was financially supported by the National Natural Science Foundation of China (No.50101009).*]

1. Introduction

The consciousness level for the fundamental importance of hygiene safety and cleanliness has been raised rapidly because of the increasing incidents caused by the spread of injurious germs. In response to such social circumstances, many antibacterial products, such as sanitation fixtures, plastic products, and articles of clothing, have been developed for use in various fields [1], and studies of stainless steel (SS) with antibacterial activity have been paid more and more attention [2-3]. To prepare a metallic material with antibacterial properties, it is not sufficient to just add antibacterial elements such as copper, silver, zinc, but annealing treatment is also necessary. Annealing treatment can make the antibacterial phase precipitate stably and disperse finely in the metallic material. For SS bearing copper, the antibacterial phase is called the copper-rich phase [4].

Ion implantation is a promising technique for solving many problems associated with surface degradation (wear, corrosion, fatigue, *etc*.) [5-7]. It is practical to produce high-value materials by ion implantation; for example, a new type of drill bit has been developed by Beijing Normal University using this method, and >5800000 pieces have been exported annually [8]. Copper implantation into SS can maintain its original characteristics and save natural resources compared with the standard method of steel production.

This study was designed to examine the ability to obtain antibacterial SS by copper ion implantation and subsequent annealing treatment. The morphology and the microstructure of Cu-implanted samples with and without annealing treatment were revealed by glancing X-ray diffraction (GXRD) and transmission electron microscopy (TEM), and the depth distributions of elements in the surface layer were obtained by Auger electron spectroscopy (AES). The corrosion-resistance of antibacterial SS was investigated by the salt wetting-drying combined cyclic corrosion test. The changes in bacterial appearance on un-implanted and annealed SS were observed by TEM and the underlying antibacterial mechanisms were discussed.

Corresponding author: Juan Xiong, **E-mail:** xiongjuana@163.com

Also available online at www.sciencedirect.com

2. Experimental

2.1. Copper ion implantation

In this study, metal vapor vacuum arc ion sources were used for the implantation of copper ions into AISI austenitic SS. Before implantation, specimens (ϕ20 mm×5 mm) were polished mechanically to a mirror finish, cleaned in acetone, and dried thoroughly. The implantation doses of ions were in the range of (0.5-8.0)×10^{17} cm^{-2}. The extracting voltage of copper implantation was 50 kV and the extracted copper ions were Cu^{2+}. Table 1 gives the implantation conditions. After ion implantation, half of the Cu-implanted specimens were annealed at 500°C for 4 h in an Ar atmosphere furnace.

Table 1. Implantation conditions

Specimen	Ions dose / (10^{17} cm^{-2})	Beam current density / (μA·cm^{-2})	Implantation Time / min
A_0	0	0	0
A_1	0.5	22	15
A_2	1.0	31	25
A_3	2.0	34	60
A_4	5.0	36	120
A_5	8.0	37	150

Antibacterial tests were performed with standard Gram-negative bacteria *Escherichia coli* (*E. coli*) ATCC25922 and Gram-positive bacteria *Staphylococcus aureus* (*S. aureus*) ATCC25923. Their antibacterial rates were calculated by the method of counting lawn [9].

2.2. Surface characterization

The phase composition of the implanted layer was determined by GXRD with Cu $K_{\alpha 1}$ (λ=0.154 nm) radiation on an X'Pert Pro diffraction instrument. The precipitated phase morphology of the annealed Cu-implanted specimens was observed with a JEM-2010 (HT) TEM with a voltage of 200 kV. The depth and the concentration profiles of elements in the layer were analyzed by PHI-610/SAM AES. The primary electronic energy of the Ar gun was 3 keV; the beam current was 25 mA, and the sputtering rate was 40 nm·min^{-1}.

2.3. Corrosion resistance

The corrosion-resistance of un-implanted SS, implanted SS, and annealed Cu-implanted SS was evaluated by the salt wetting-drying combined cyclic corrosion test using 5 cycles and each cycle was implemented as follows.

(1) Spraying 3.5wt% NaCl solution onto the surface of specimens for 0.5 h;

(2) Drying specimens at 60°C for 1 h;

(3) Keeping specimens for 1 h in an atmosphere of >95% relative humidity.

The surface appearance and the percentages of pitting corrosion area were obtained by optical microscopy and the micro-image analysis and process system, respectively.

3. Results

3.1. Antibacterial property analysis

Table 2 gives the antibacterial test results of un-implanted SS and Cu-implanted SS with and without annealing treatment. It can be seen that the antibacterial rate of un-implanted SS was zero, that is, had no antibacterial property. The antibacterial rates of Cu-implanted specimens against *E. coli* were above 99% when the implantation dose of ions was >1.0×10^{17} cm^{-2}, irrespective of whether the specimens were annealed or not. However, all specimens without annealing treatment did not have a good antibacterial property against *S. aureus*. After annealing treatment, Cu-implanted specimens had a good antibacterial property against *E. coli* and the antibacterial rates against *S. aureus* were increased. When the specimen was implanted with an ions dose of 8.0×10^{17} cm^{-2} and was annealed, the antibacterial rates were 100% against both *E. coli* and *S. aureus*.

Table 2. Antibacterial results

Specimen	Annealing treatment	Antibacterial rate / %	
		E. coli 4.2×10^5 cfu/mL	*S. aureus* 7.5×10^5 cfu/mL
A_0	Without	0	0
	With	0	0
A_1	Without	80.7	23.4
	With	99.5	58.5
A_2	Without	99.8	40.3
	With	99.8	72.7
A_3	Without	100	52.9
	With	100	80.0
A_4	Without	100	54.1
	With	100	95.3
A_5	Without	100	80.4
	With	100	100

Note: cfu denotes colony-forming unit; cfu/ml is the unit for concentration of bacteria.

The difference in antibacterial property against *E. coli* and *S. aureus* is related to two aspects. One is the implantation dose, which will be discussed later. The other is the different physical structures of *E. coli* and *S. aureus*. Yokota *et al*. [10] proposed that the mechanism of Cu ions in antibacterial activity consists of the

following two steps. First, Cu ions eluted from the surface of the material adhere to the surface of the bacterial cells in a humid atmosphere; second, Cu ions damage the cell membrane and solidify the structure of proteins. So, the antibacterial property depends crucially on whether copper ions can penetrate the cell membrane. From Fig. 1, the thickness of the cell wall of *E. coli* is 2-3 nm; however, the thickness of the cell wall of *S. aureus* is 20-80 nm [11]. The cell wall of *S. aureus* is thicker than that of *E. coli*, and it is more difficult for copper ions to penetrate the cell to kill *S. aureus*.

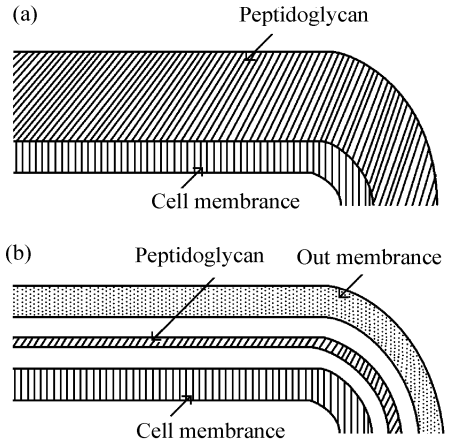

Fig. 1. Structures of the cell wall of the two kinds of bacteria: (a) *E. coli*; (b) *S. aureus*.

3.2. Microstructures of antibacterial SS in the implanted layer

GXRD at an incident angle of 1° was used to examine the phase composition in the surface layer. Fig. 2 shows the GXRD patterns of Cu-implanted specimen A_5 with and without annealing treatment. Fig. 2(a) shows that the new phase $Cu_{9.9}Fe_{0.1}$ was found in the surface layer of the Cu-implantation specimen without annealing treatment as well as the austenitic substrate γ-Fe. Another new phase Fe-Cr resulting from precipitated chrome, which then formed a substitution solid solution during copper ion implantation, was found in the surface layer [12].

After annealing treatment, the copper-rich phase $Cu_{9.9}Fe_{0.1}$ was still present, but the Fe-Cr phase had disappeared (in Fig. 2(b)). The reason for the disappearance of the Fe-Cr phase is that chrome elements solute into the austenitic substrate again during annealing treatment at 500°C for 4 h. In Fig. 2(b), Fe_4O_3 is present in the implanted layer. It is because the vacuum level was not very high in the Ar atmosphere furnace, which caused the surface of the specimen to be oxidized at high temperature over several hours.

The GXRD results show that the Cu-rich phase existed as a form of $Cu_{9.9}Fe_{0.1}$ in Cu-implanted specimens with and without annealing treatment.

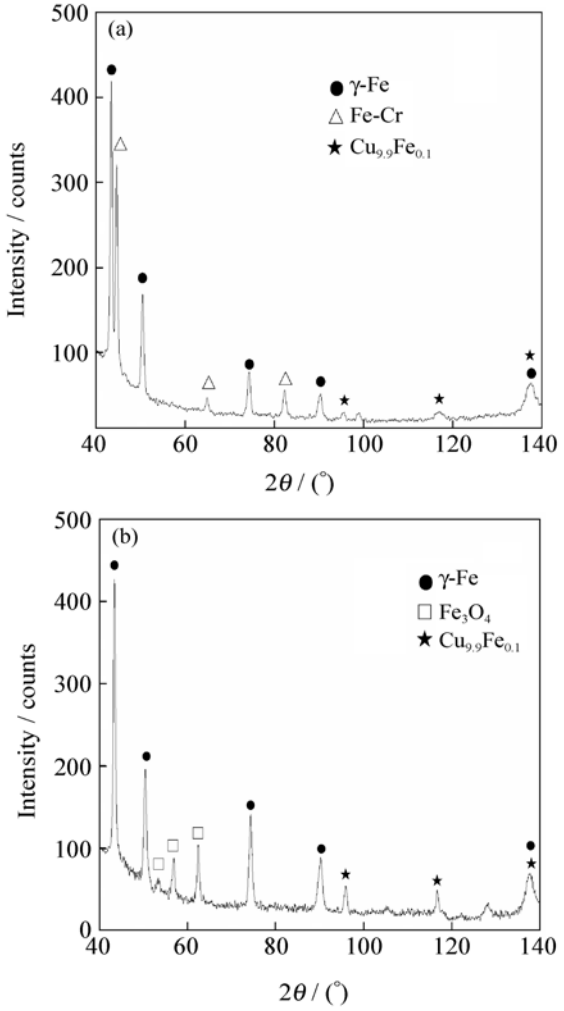

Fig. 2. GXRD patterns of specimen A_5: (a) without annealing treatment; (b) with annealing treatment.

3.3. TEM analysis of the surface layer

The surface views of un-implanted specimen A_0 and Cu-implanted specimen A_5 with annealing treatment were observed by TEM. Figs. 3 and 4 show the difference of diffraction patterns between un-implanted SS and antibacterial SS, respectively. Fig. 3 reveals the morphology and corresponding diffraction pattern of γ-Fe in the un-implanted SS, but in Fig. 4(a), cluster structure and the needle-precipitation in the middle of the cluster structure appear in specimen A_5 after annealing treatment. The selected area diffraction (SAD) patterns of the needle-precipitation and standardization (Fig. 4(b)) testify that the needle-precipitation is $Cu_{9.9}Fe_{0.1}$, which agrees with the GXRD results.

3.4. Distribution of elements in the surface layer

The AES depth profiles of Cu-implanted specimen A_5 with and without annealing treatment are summarized in Fig. 5. As shown in Fig. 5(a), copper does not been found after 3.0 min before annealing treatment.

According to the sputtering rate of 40 nm·min^{-1}, the depth of copper in the implanted layer was about 120 nm and its peak value was 28at%. From Fig. 5(b), it can be seen that after annealing treatment, the copper concentration profile became smooth and homogeneous. The average concentration of copper in the surface layer was 10at%, and the layer deepened to about 400 nm. This phenomenon showed that the copper atoms diffused into the SS after annealing treatment. Compared with the specimen without annealing treatment, the depth of the copper-rich phase increased and its concentration decreased in the surface layer after annealing treatment, It is also noted that a concentration of 10at% for the copper-rich phase was enough to produce a specimen with good antibacterial property.

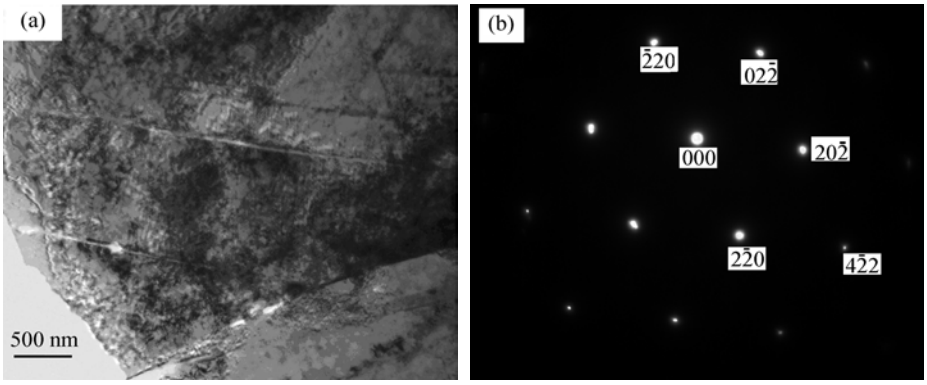

Fig. 3. TEM morphology of un-implanted specimen A_0: (a) TEM image of γ-Fe; (b) diffraction patterns and standardization of the patterns.

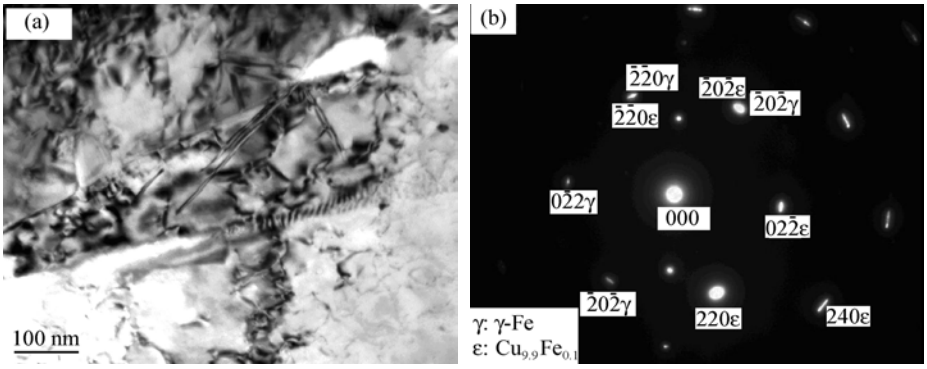

Fig. 4. TEM surface view of Cu-implanted specimen A_5 with annealing treatment: (a) TEM image of Cu-rich phase; (b) SAD patterns and standardization of the patterns.

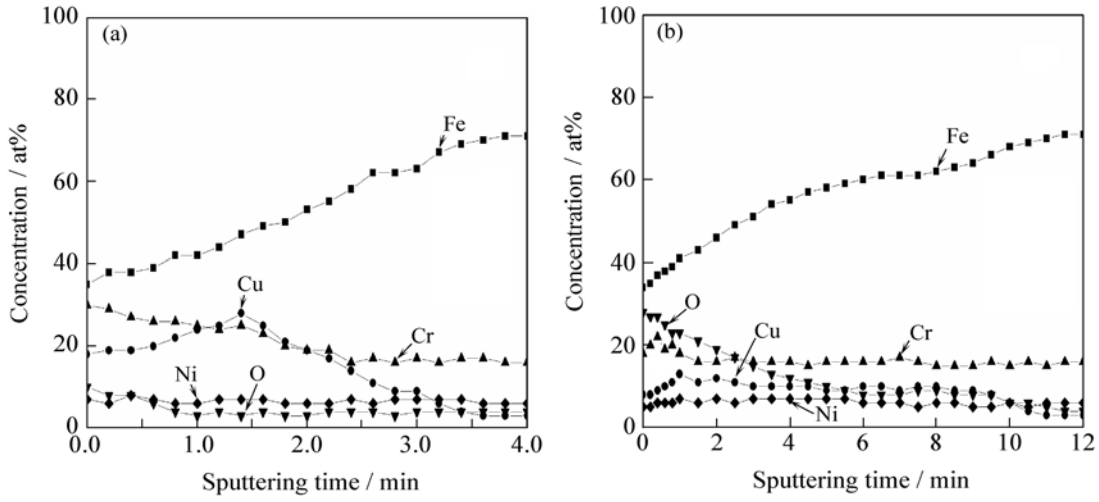

Fig. 5. Concentration profiles of Cu-implanted specimen A_5 by AES: (a) without annealing treatment; (b) with annealing treatment.

AES tests show that chrome migrated to the specimen surface after implantation and became homogeneous after annealing treatment. This phenomenon verified the appearance and disappearance of Fe-Cr in GXRD. It can be seen from Fig. 5 that the implanted specimen contained a certain amount of oxygen, espe-

cially in the annealed specimen, because the degree of vacuum during implantation was not high, and the SS surface was oxidized during the annealing process.

The AES results show that copper ions were distributed in the area near the SS surface after implantation, and then diffuse into the inner section after annealing treatment.

3.5. Corrosion-resistance of antibacterial SS

The surface appearances of common SS and Cu-implanted specimens with and without annealing treatment after 5 cycles of salt wetting-drying are shown in Fig. 6. Table 3 shows the percentage of rusty area accounted by the method of metallographic quantitative analysis. As shown in Table 3, the corrosion resistance of Cu-implanted specimens with and without annealing treatment changes slightly, so the antibacterial SS has a level of corrosion resistance equivalent to that of common AISI 304 SS.

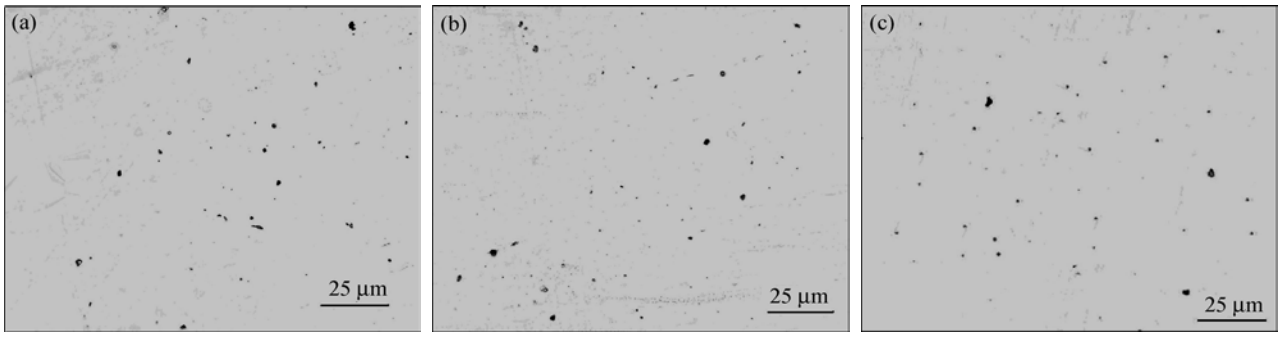

Fig. 6. Morphologies on the surface of specimens after 5 cycles of salt wetting–drying: (a) common SS; (b) Cu-implanted specimen without annealing treatment; (c) Cu-implanted specimen with annealing treatment.

Table 3. Percentage of pitting corrosion area

Treatment condition	Pitting corrosion areas / %
Common stainless steel	1.7±0.1
Cu-implanted without annealing treatment	1.6±0.1
Cu-implanted with annealing treatment	1.8±0.1

4. Discussion

4.1. Effect of implantation dose and annealing treatment on antibacterial property

Metallic elements containing silver and copper have favorable effects on antibacterial property [10]. Copper has good antibacterial activity when it exists as a Cu-rich phase and is distributed homogeneously in a solid solution. The antibacterial property of SS depends highly on the form of copper in the material.

It can be seen from Table 2 that the antibacterial rates against *E. coli* and *S. aureus* increased with increasing implantation dose. After the implantation of copper ions, the antibacterial rates against *S. aureus* increased from 23% to 80% with the increased doses of ions from 5.0×10^{16} to 8.0×10^{17} cm^{-2}. The antibacterial property is related to the concentration of the copper-rich phase in the implanted layer. When the implantation dose is lower than 8.0×10^{17} cm^{-2}, the content of the copper-rich phase is not sufficient to show antibacterial activity. It can be seen from Fig. 5 that the specimen had excellent antibacterial properties against both *E. coli* and *S. aureus* only when the specimen was implanted with an ion dose of 8.0×10^{17} cm^{-2} and the concentration of the copper-rich phase was 10at%.

Figs. 2 and 4 show that copper exists as a copper-rich phase of $Cu_{9.9}Fe_{0.1}$ in Cu-implanted SS with and without annealing treatment. Fig. 5(a) shows that copper was distributed in the area near the SS surface. After annealing treatment, copper element diffused into the inner area in SS, so the copper-rich phase was distributed more homogeneously than in SS without annealing treatment. Although the concentration of copper in the specimen without annealing treatment (28at%) was higher than that in the specimen with annealing treatment, its distribution was not more homogeneous and was not deeper than the latter (10at%). The specimen had good antibacterial property against only *E. coli*. On the other hand, the Fe-Cr phase appeared after implantation and disappeared after annealing treatment, which is shown in Fig. 2. It is the Fe-Cr phase that holds back the precipitation of copper that results in the degradation of the antibacterial activity of $Cu_{9.9}Fe_{0.1}$, so the antibacterial property against *S. aureus* is unfavorable. Chrome solutes passed unhindered into the substrate, the Fe-Cr phase disappeared and $Cu_{9.9}Fe_{0.1}$ precipitated from the surface layer after annealing treatment, so the SS exhibited antibacterial property against both *E. coli* and *S. aureus*.

The above discussion makes it clear that the copper-rich phase was distributed homogeneously and without hindrance by Fe-Cr only when the specimen

with an ions implantation dose of 8.0×10^{17} cm^{-2} and subsequent annealing treatment, and this SS showed excellent antibacterial property against both *E. coli* and *S. aureus*. This confirms that annealing treatment is an indispensable step to improve the antibacterial property of the Cu-implanted specimen.

4.2. Effects of implantation and annealing treatment on corrosive property

It is well known that chromium is the critical element in SS that helps improve the corrosion resistance [13]. Fig. 5 shows that the concentration of chromium in the implanted layer of specimen A_5 was higher than that in un-implanted SS. But the concentration of chromium in the implanted layer remained at 18at% after annealing treatment, which is almost equivalent to the concentration in un-implanted SS. The increase in concentration of chromium in the implanted layer is because of the Fe-Cr phase formation, as shown in Fig. 4. After annealing treatment, Fe-Cr disappeared, so the concentration of chromium was equivalent to the original concentration of un-implanted SS.

In summary, antibacterial SS has a level of corrosion resistance equal to that of common AISI 304 SS.

5. Conclusion

AISI 304 austenitic SS displays excellent antibacterial property against both *E. coli* and *S. aureus* when it was implanted by an ion dose of 8.0×10^{17} cm^{-2} and subsequently given an annealing treatment. The presence of the copper-rich phase in the surface layer contributes to the excellent antibacterial property of SS. The copper-rich phase $Cu_{9.9}Fe_{0.1}$ precipitates as needles in the surface layer after copper ion implantation and annealing treatment. The concentration of copper is 28at% and the depth is about 120 nm after the implantation; after annealing treatment, the concentration becomes 10at%, and the depth of copper increases to 400 nm, so the copper-rich phase is distributed homogeneously and the Fe-Cr phase disappears, which helps the unhindered precipitation of $Cu_{9.9}Fe_{0.1}$. The corrosion resistance level of antibacterial SS is equivalent to that of common AISI 304 SS. The annealed Cu-implanted SS has excellent antibacterial property and has a level of corrosion resistance equal to that of common AISI 304 SS.

References

[1] W. Zhang and P.K. Chu, Enhancement of antibacterial properties and biocompatibility of polyethylene by silver and copper plasma immersion ion implantation, *Surf. Coat. Technol*., 203(2008), No.5-7, p.909.

[2] I.T. Hong and C.H. Koo, Antibacterial properties, corrosion resistance and mechanical properties of Cu-modified SUS 304 stainless steel, *Mater. Sci. Eng. A*, 393(2005), No.1-2, p.213.

[3] D.P. Dowling, K. Donnelly, M.L. McConnell, R. Eloy, and M.N. Arnaud, Deposition of anti-bacterial silver coatings on polymeric substrates, *Thin Solid Films*, 398(2001), No.1-2, p.602.

[4] N. Ooknbo and S.N. Masato, Antimicrobial activity and basic properties of antimicrobial stainless steel, *Nisshin Steel Tech. Rep.*, 77(1998), No.11, p.69.

[5] S. Mändl, B. Fritzsche, and D. Manova, Wear reduction in AISI 630 martensitic stainless steel after energetic nitrogen ion implantation, *Surf. Coat. Technol.*, 195(2005), No.2-3, p.258.

[6] E. Cano, L. Martínez, J. Simancas, F.J. Pérez-Trujillo, C. Gómez, and J.M. Bastidas, Influence of N, Ar and Si ion implantation on the passive layer and corrosion behaviour of AISI 304 and 430 stainless steels, *Surf. Coat. Technol.*, 200(2006), No.16-17, p.5123.

[7] J.P. Riviere, P. Meheust, and J.P. Villain, High current density nitrogen implantation of an austenitic stainless steel, *Surf. Coat. Technol.*, 158-159(2002), No.12, p.99.

[8] T.H. Zhang and Y.G. Wu, New development trend of ion beam modification of materials, *Nucl. Tech.* (in Chinese), 21(1998), No.12, p.752.

[9] W.Y. Han, *Pathogenic Bacteria Testing Technology*, Jilin Science and Technology Press, Jilin, 1992, p.79.

[10] T. Yokota, M. Tochibara, and M. Ohta, Silver dispersed stainless steel with antibacterial property, *Kawasaki Steel Tech. Rep.* (in Japanese), 46(2002), No.8, p.37.

[11] Z.G. Dan, H.W. Ni, and B.F. Xu, Microstructure and antibacterial properties of AISI 420 stainless steel implanted by copper ions, *Thin Solid Films*, 492(2005), No.1-2, p.93.

[12] D. Manova, D. Hirsch, J.W. Gerlach, T. Höche, S. Mändl, and H. Neumann, Nitriding of Fe-Cr-Ni films by low energy ion implantation, *Surf. Coat. Technol.*, 202(2008), No.11, p.2443.

[13] D.Q. Peng, X.D. Bai, R.H. Yu, and X.W. Chen, Role of chromium ion implantation on the corrosion behavior of zirconium in 1 N H_2SO_4, *Appl. Surf. Sci.*, 230(2004), No.1-4, p.73.